Supplemental material for 'Parametric numerical study of passive scalar mixing in shock turbulence interaction'

Xiangyu Gao[1]†, Ivan Bermejo-Moreno[1]‡, and Johan Larsson[2]

[1]Aerospace and Mechanical Engineering Department, University of Southern California, Los Angeles, CA 90089, USA

[2]Mechanical Engineering Department, University of Maryland, College Park, MD 20742, USA

1. Verification

The grids used in the present simulations are stretched such that the resolution is highest near the shock, where the Kolmogorov scale is the smallest (Larsson & Lele 2009). Figure 1 shows profiles of the grid spacing in the mean shock-normal direction for different simulations along with profiles of $k_{\max}\eta$, exceeding unity at all locations. Grid convergence of statistics is assessed by comparing results from series of simulations run at increasing grid resolution for different combinations of dimensionless parameters. Figure 2 shows Kolmogorov scale, transverse vorticity variance, passive scalar variance (for $Sc = 1$) and scalar dissipation for case $(M, M_t, Re_\lambda) = (2.0, 0.3, 38)$, comparing results obtained from four independent simulations performed at increasing resolution: 426×128^2, 852×256^2, 1280×384^2, 1700×512^2 (case F on table 1). Differences between the 1280×384^2 and 1700×512^2 grids are less than 1% for all statistics, including background turbulent flow quantities and those of the passive scalar. Thus, the 1280×384^2 simulations are deemed grid-converged. A similar analysis is presented for simulations at the highest Reynolds number considered in this study. Figure 3 shows results for simulations with $(M, M_t, Re_\lambda) = (5.0, 0.3, 72)$ at resolutions 600×256^2, 1200×512^2, 1800×768^2, and 2400×1024^2 in which the convergence of statistics can also be observed.

The effects of using a finite computational box size and varying the wavenumber at which the energy peaks, k_0, were discussed in Larsson, Bermejo-Moreno & Lele (2013). In the present simulations we choose the same box size, $4\pi \times (2\pi)^2$, and peak-energy mode $k_0 = 4$, which were shown to have a minimal influence on the simulation results.

Another relevant metric to examine the convergence of averaged simulation results is the difference between the sum of all terms on the left and right hand sides of each transport equation presented in §3.1. Figure 4(a) shows the streamwise profiles of non-negligible terms in the scalar variance transport equation as well as the total contribution from the left- and right-hand sides, for a representative case at $(M, M_t, Re_\lambda) = (1.28, 0.31, 41)$. Figure 4($b$) shows equivalent results for the scalar dissipation transport equation. In both cases, the difference between each side of the equation is negligible. However, convergence of the left and right hand sides of the scalar dissipation transport equation generally requires an additional level of refinement compared with the other statistics, as it involves higher-order spatial derivatives (notice the $1700 \times 512 \times 512$ grid resolution of the simulation used for that figure).

† Email address for correspondence: xiangyug@usc.edu
‡ Email address for correspondence: bermejom@usc.edu

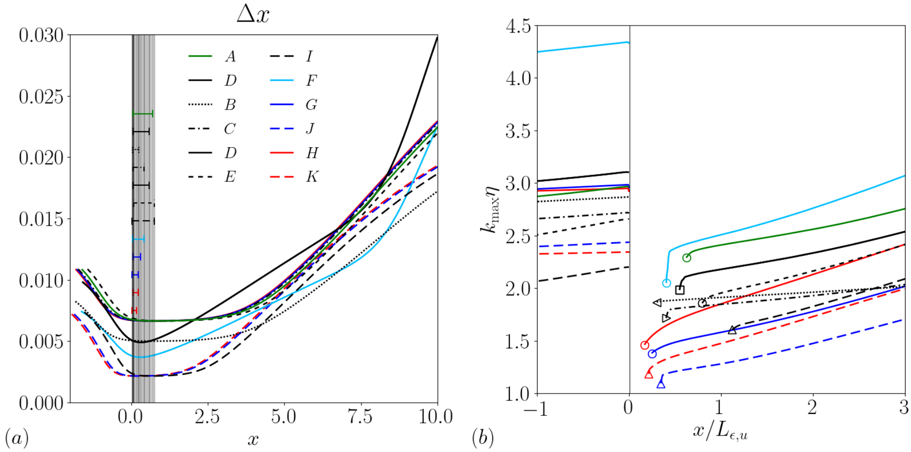

Figure 1: (a) Streamwise grid spacing and (b) $k_{\max}\eta$ profiles for all the cases in table 1.

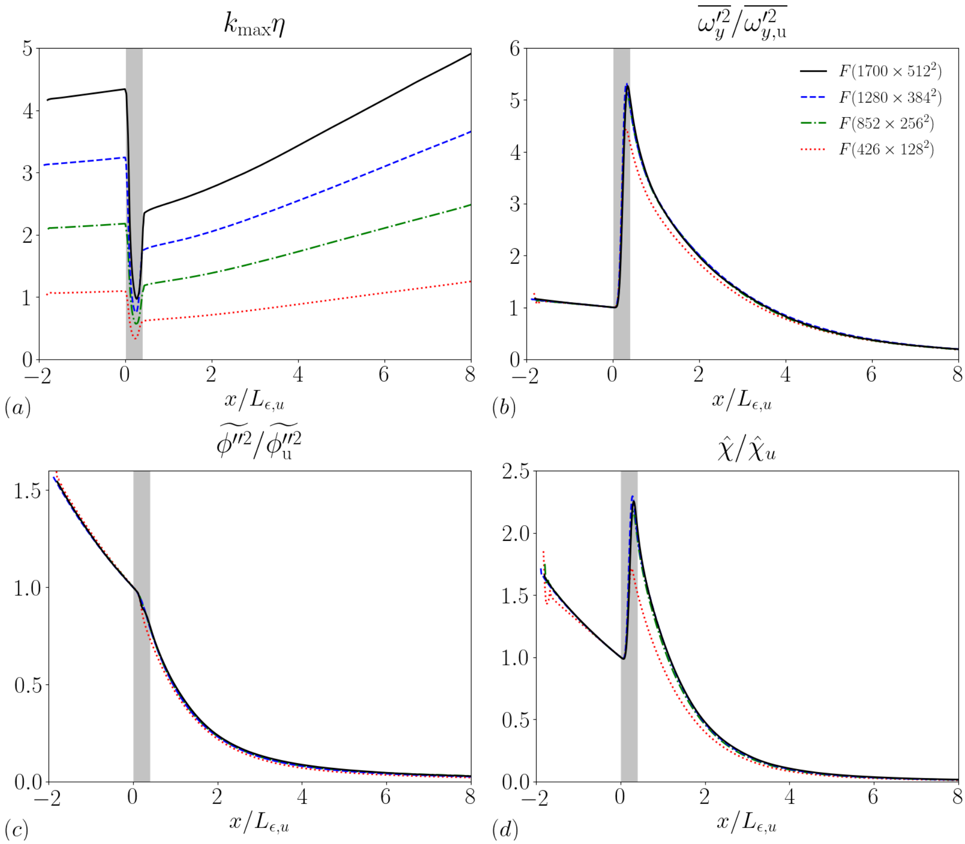

Figure 2: Grid convergence test for case F, with $(M, M_t, Re_\lambda) = (2.0, 0.3, 40)$ on increasingly finer grids: 426×128^2 (dotted), 852×256^2 (dash-dotted), 1280×384^2 (dashed), 1700×512^2 (solid). (a) $k_{\max}\eta$, (b) transverse vorticity variance $\overline{\omega_2'\omega_2'}$. ($c$) scalar variance, $\widetilde{\phi''^2}$ (d) scalar dissipation rate, $\hat{\chi}$. Quantities in (b)-(d) are normalized with their corresponding value immediately upstream of the shock.

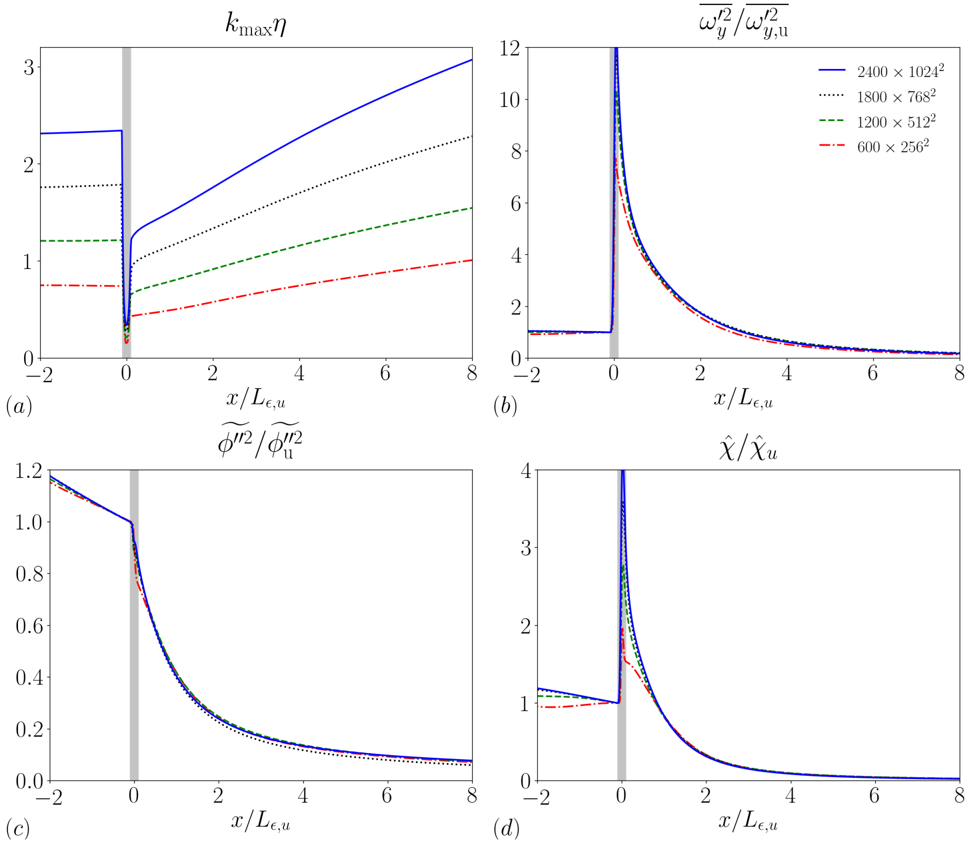

Figure 3: Grid convergence test for case K, with $(M, M_t, Re_\lambda) = (5.0, 0.3, 72)$ on increasingly finer grids: 600×256^2 (dotted), 1200×512^2 (dash-dotted), 1800×768^2 (dashed), 2400×1024^2 (solid). (a) $k_{\max}\eta$, (b) transverse vorticity variance $\overline{\omega'_2\omega'_2}$. (c) scalar variance, (d) scalar dissipation rate, $\hat{\chi}$. Normalizations as in figure 2.

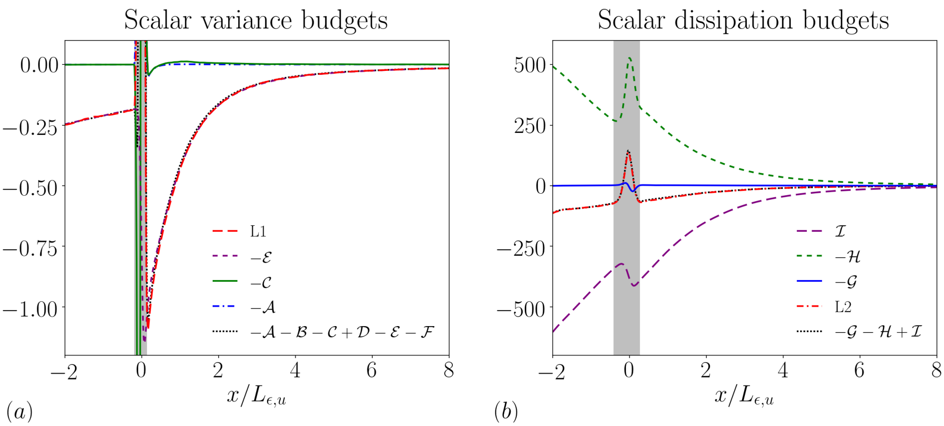

Figure 4: Streamwise profiles comparing left- and right-hand side terms of (a) scalar variance transport equation (3.2) for case J and (b) scalar dissipation transport equation 3.1) for case A (at a higher resolution of $1700 \times 512 \times 512$).